SUPPORTING INFORMATION

Chiral Induction at the Nanoscale and Spin Selectivity in Electron Transmission in Chiral Methylated BEDT-TTF derivatives

Alberta Carella,[1] Suryakant Mishra,[2] Camilla Ferrari,[3] Davide Vanossi,[4] Francesco Rossella,[1] Flavia Pop,[5] Narcis Avarvari,[5*] Han Htoon,[2] Jennifer A. Hollingsworth,[2] Eric G. Bowes,[2] Somak Majumder,[2] Andrew Crandall Jones[2*] and Claudio Fontanesi[3*]

[1]Department of Physics, FIM, University of Modena and Reggio Emilia, via Campi 213, 41125 Modena, Italy

[2]Center for Integrated Nanotechnologies, Los Alamos National Laboratory, Los Alamos, New Mexico, USA

[3]Department of Engineering "Enzo Ferrari", (DIEF), Univ. of Modena, Via Vivarelli 10, 41125 Modena, Italy.

[4]Department of Chemistry, DSCG, University of Modena and Reggio Emilia, via Campi 183, gg41125, Modena, Italy

[5]Univ Angers, CNRS, MOLTECH-Anjou, SFR MATRIX, F-49000 Angers, France.

Correspondance
Narcis Avarvari: narcis.avarvari@univ-angers.fr
Andrew Crandall Jones: acj@lanl.gov
Claudio Fontanesi: claudio.fontanesi@unimore.it

INDEX

1. Photoluminescence (PL)

5 nm of titanium and 150 nm of nickel were deposited on a 200 nm SiO_2-on-Si (100) wafer substrate by the electron beam evaporation technique in a clean room. A suspension of **1** (Tetramethyl-Bis(ethylenedithio)-Tetrathiafulvalene, the relevant structure is shown in the main manuscript) crystals (0.4 mM) has been prepared in ethanol and mixed with a hexane suspension of CdSe@CdS QDs. QDs were uniformly spincast from a suspension of **1** crystals mixed with the QDs suspension in hexane from a dilute solution to yield eventually an average concentration in between 1 to 3 ML. After ultrasonication, the resulting mixture was dropcasted on the clean Ni(150 nm)/Ti(5 nm) surface (Figure S1). QD light emitters were photoexcited above the relevant bandgap by using a linearly polarized pulsed laser source operating at ~3 eV (405 nm). The degree of circular polarization of the photoluminescence emission from the quantum dots was resolved using a Wollaston prism in the detection beampath prior to spectral characterization. Individual quantum dot emitters were spotted exploiting widefield illumination imaging.

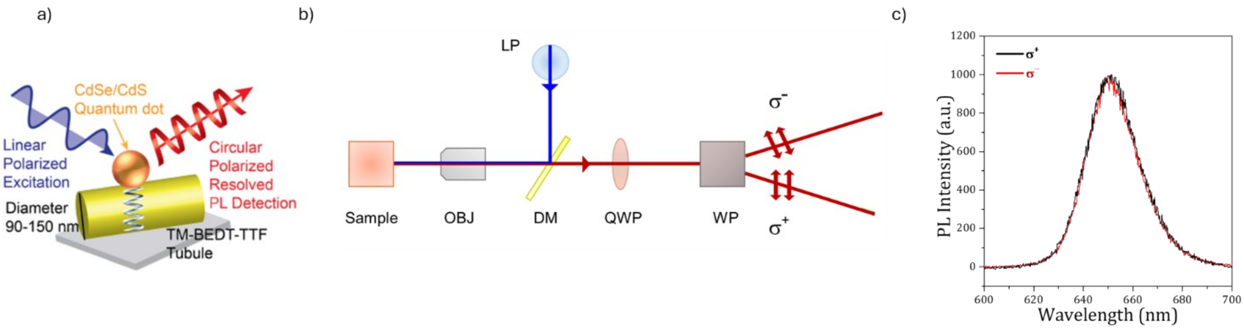

Figure S1. a) Circularly polarized luminescence (CPL) sample schematic representation: the sphere on top represents the QD, standing on top of the enantiopure **1** crystal (represented as a spring-helix), the substrate is nickel. b) Schematic of optical setup for the measurement of circular polarization-resolved photoluminescence emission. In order, the acronyms stand for:OBJ = objective, LP = linear polarizer; DM = dichroic mirror; QWP = quarter-wave plate; WP = Wollaston prism. c) Control measurement of bare QDs on cover slip in the absence of a chiral system. Here, the PL data shows no degree of circularly polarized emission.

As evidence of the CISS effect, the influence of chirality on the variation of the degree of circular polarization (DCP) of photoluminescence from single emitters was analyzed, magnetizing the Ni surface out-of-plane and in-plane respectively, and collecting in this way polarization-resolved PL measurements. As supposed, the effect of magnetization on the DCP switched in the two cases.

2. Ni substrate characterization

5nm Titanium and 150nm Nickel was deposited on a 200nm SiO_2-on-Si (100) wafer substrate using e-beam evaporation in a clean room. Figure S2 shows the morphology of the Ni substrate used in this work. Mean roughness calculated: 106.1 pm

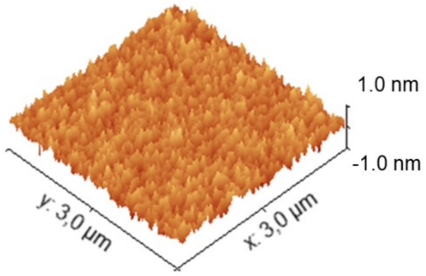

S2. Topographic map of Nickel substrate.

3. Electrochemistry results

In Figure S3 it is reported the cyclic voltammetry (CV) of 1 in a solution of ACN with TBATFB 0.1M. Both enantiomers have similar behavior. CV shows a first peak couple at 0.49 - 0.57 V, where the small separation in potential indicates a fully reversible reaction. A second peak couple is at 0.76-0.90V, since they are more distant in potential the process is less reversible; the third process shows a clear peak in oxidation at 1.20 V and only a shoulder at 1.08 V in the more positive potential domain (oxidation regime) part of the voltammetry, indicating a non-reversible process.

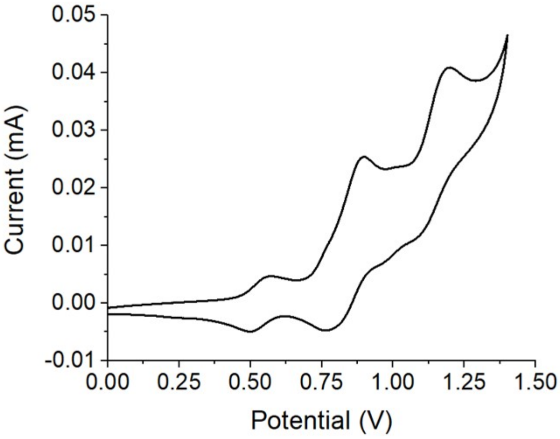

Fig.S3 Cyclic voltammetry of **1**, 5 mM concentration, in 0.1M TBATFB in ACN solution. Glassy carbon is the working electrode, a Pt sheet the counter electrode, Ag/AgCl/KCl the reference electrode, 50 mV s^{-1} is the potential scan rate.

4. CD and UV-Vis Spectra

Circular dichroism spectra of the two enantiomers are shown in Fig.S4. Both curves have a peak at 225 nm and they are equal to zero at 253 nm, while the other peak is at 275 nm and 273 nm for (S)-**1** and (R)-**1** respectively.

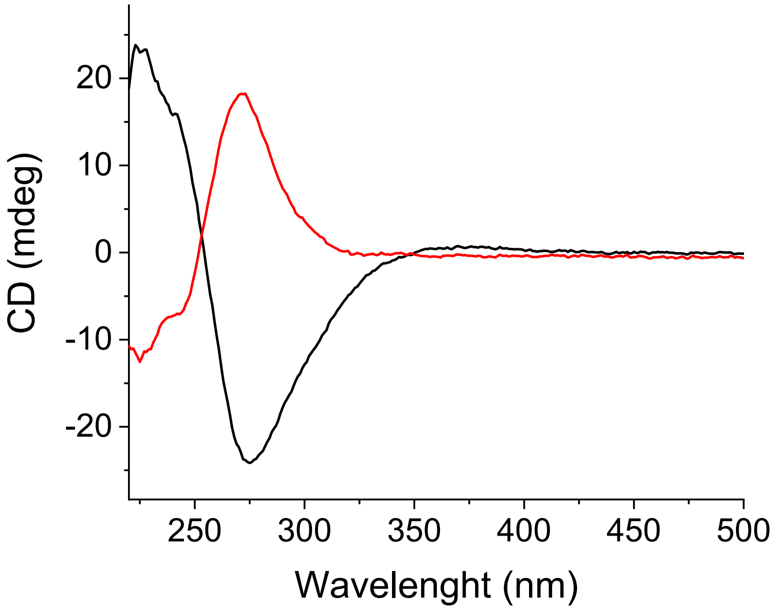

Fig.S4 Circular dichroism of (S)-**1** (black line) and (R)-**1** (red line), in ACN solution.

The electronic spectra of **1** (Fig.S5A) show for both enantiomers a strong absorption at 223 nm, and an additional peak at 304 nm with a shoulder at 347 nm. These data are in good agreement whit the results of theoretical calculation (Fig.S5B). Considering that the solvent was not taken into account, the latter showed peaks at 258 nm, 309 nm and a shoulder at 359 nm.

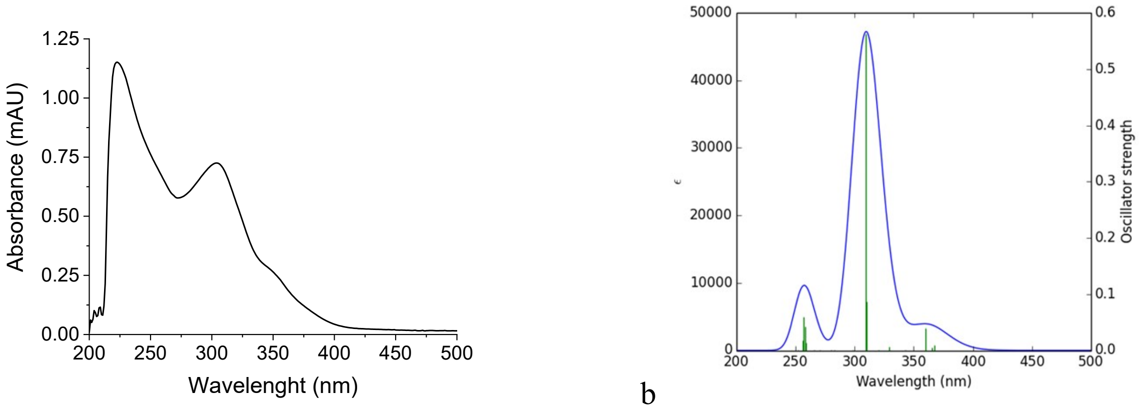

a

b

Fig.S5 a) UVvis spectra of **1** in ACN solution. b) Theoretical spectra of **1**.

5. InfraRed Spectra

GA-FT-IR spectrum of **1** pristine is shown in Fig.S6.

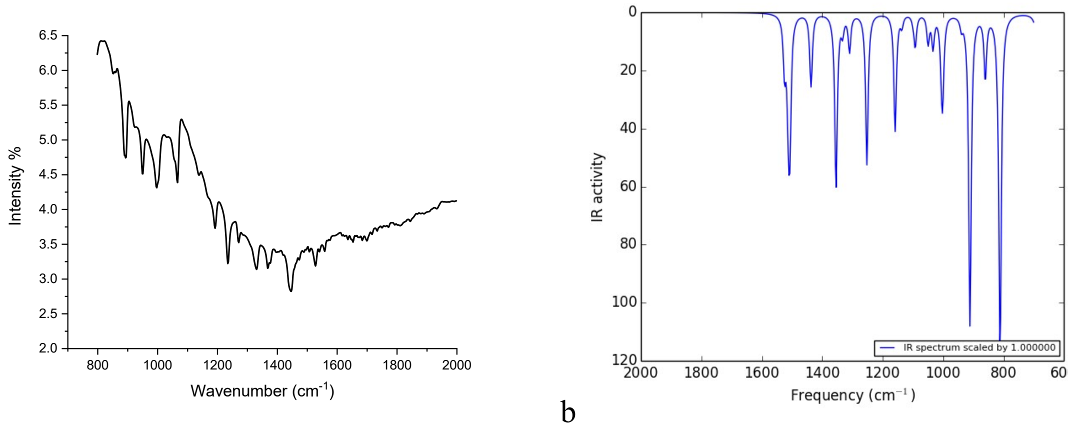

a b

Fig.S6 a) GA-FT-IR spectra recorded for pristine **1** in the 2000 – 700 cm^{-1} wavenumber range, dropcast on a Pt surface from a 5 mM solution of enantiopure **1** in DCM. b) Theoretical calculation of the IR spectra of 1.

6. Micro Raman Spectra

Micro Raman spectrum of **1** pristine is shown in Fig.S7A. The experimental spectrum is in good agreement whit the results of theoretical calculation, shown in Fig.S7B.

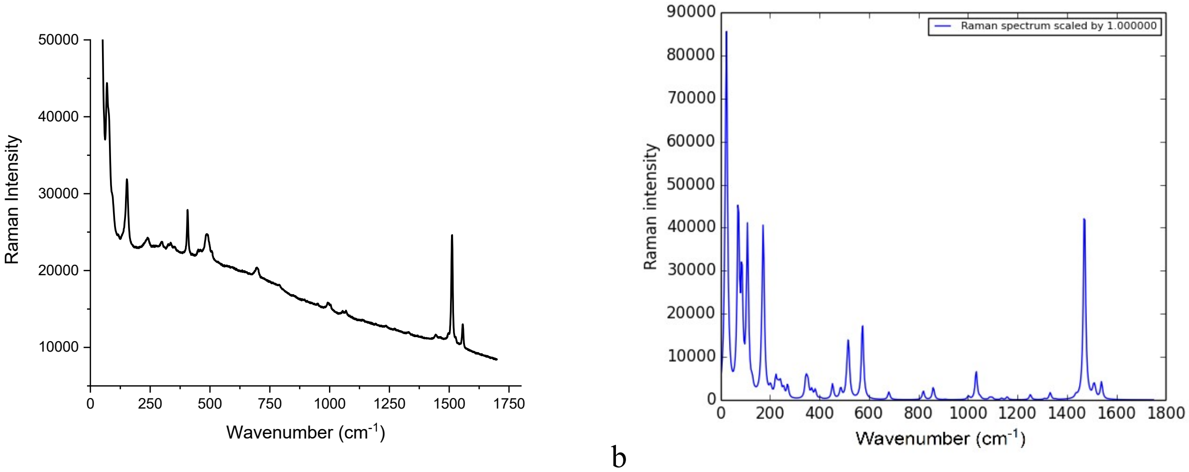

a b

Fig.S7 a) microRaman spectrum recorded at 785 nm, for pristine **1** dropcasted on a platinum surface. b) theoretical calculation of the microRaman spectra of **1**.

7. Theoretical calculations

Theoretical calculations are carried out at the semiempirical level of the theory, PM6 Hamiltonian. The choice of a semiempirical Hamiltonian (i.e. only valence electrons enter explicitly in the calculations, while core electrons are essentially treated as a core potential) is due to the large number of centers involved in the cluster (determined by the physical dimension of the QD), in addition both cadmium and selenium need to account for relativistic effects in the Hamiltonian. In addition, the rigorous calculation of emission spectra would imply to know the nature of the emitting electronic state, and also take into account its geometrical optimization (the electronic excitation can be approximate as a Frank-Condon process, so that the final excited state geometry does not correspond to the equilibrium one, please compare Figure S8) with the relevant geometrical excited state relaxation.[1]

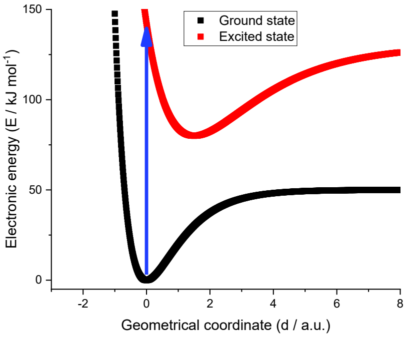

Figure S8. Schematic representation of a Franck-Condon transition. Black and red curves represent the ground and first excited state, respectively. The blue arrow represents the vertical transition from the ground state to the excited states, the latter in general is characterized by a different equilibrium geometry with respect to that of the ground state.

Details of the approximations and of the level of the theory are here listed in detail.

1) In QM calculations both Cd and Se are considered as heavy atoms, because of their large atomic number. Thus, due to the rather large number and nature of the atoms involved in the simulation of the QD: **1** cluster a rigorous ab-initio all electrons approach has to be ruled out. To keep computational costs (time) into reasonable limits, the semi-empirical PM6 Hamiltonian was selected. The latter proved to be effective in the calculation of structural and electronic properties of a wide range of organic and inorganic crystalline solids.[2]

2) The cadmium selenide slab dimensions, $Cd_{16}Se_{16}$, were selected based on the theoretical results of ref.[3] The $Cd_{16}Se_{16}$geometrical coordinates are obtained by the experimental solid state X-ray analysis results,[4] see the 9016056.cif file, from crystal open database archive (COD: https://www.crystallography.net/cod/), Figure S9. An approximation in QM calculations concerns the geometrical coordinates of the $Cd_{16}Se_{16}$, which are kept fixed, so to maintain the basic structure of the crystal. Finally, the $Cd_{16}Se_{16}$ slab is assumed to be representative of the electronic properties of the QD.

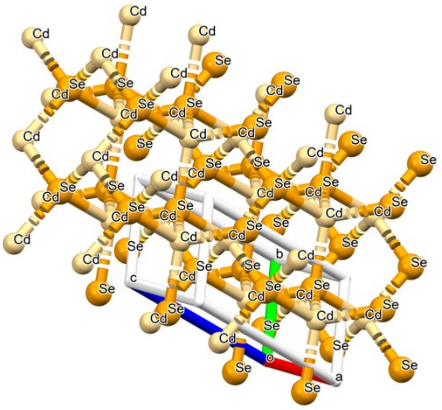

Figure S9. CdSe crystal 2x2x2 supercell representation, 9016056.cif file.[4]

3) The QD: $Cd_{16}Se_{16}$ cluster geometry is then obtained by a full optimization of the geometrical coordinates of **1**, including the intermolecular **1** to QD distance and angle of interaction. The $Cd_{18}Se_{18}$ geometry is maintained fixed. This approach also allowed to determine the intermolecular energy interaction between QD and **1** in the cluster, which is found just slightly smaller than the experimental one.[5]

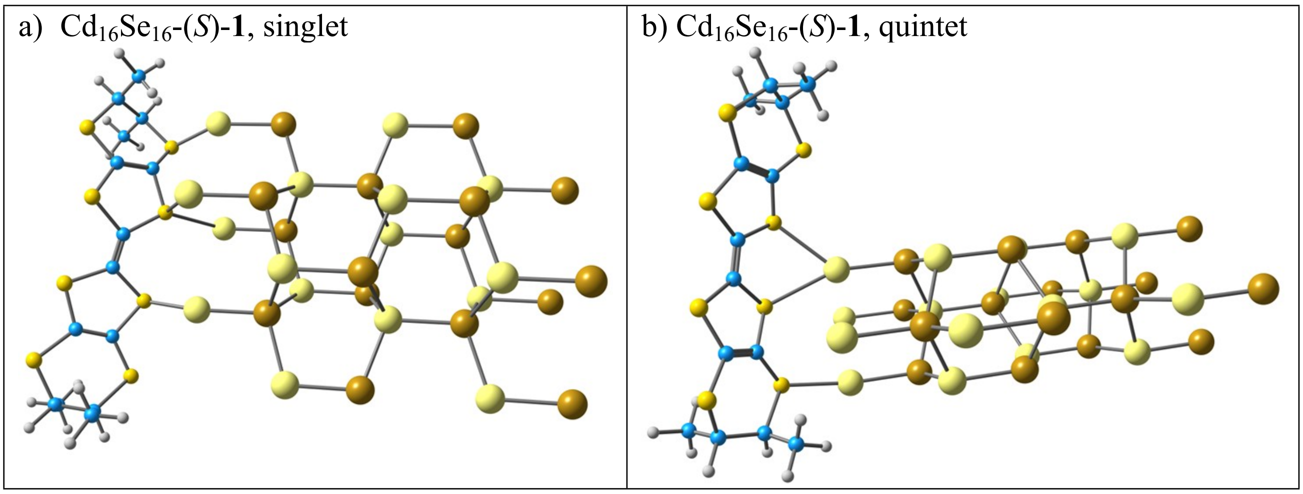

a) $Cd_{16}Se_{16}$-(*S*)-**1**, singlet

b) $Cd_{16}Se_{16}$-(*S*)-**1**, quintet

Figure S10. a) $Cd_{16}Se_{16}$:(*S*)-**1** cluster molecular structure, singlet electronic state, obtained after PM6 geometrical optimization. b) $Cd_{16}Se_{16}$:(*S*)-**1** cluster molecular structure, quintet electronic state, obtained after PM6 geometrical optimization. Colour code used for the atoms is yellow for sulphur, turquoise for carbon, grey for hydrogen, bright yellow larger sphere for cadmium and brown larger sphere for selenium.

$Cd_{16}Se_{16}$-(*S*)-**1** cartesian coordinates following PM6 partial optimization, singlet, triplet and quintet electronic states.

Figure S10a cartesian coordinates $Cd_{16}Se_{16}$-(*S*)-**1** singlet PM6 partial optimization:

Cd	-4.953685000	-0.997899000	-2.106040000
Se	-2.318580000	-1.178540000	-2.112395000
Cd	-1.287298000	1.238161000	-2.162582000
Se	1.347806000	1.057520000	-2.168938000

Cd	2.039881000	-1.477322000	-2.122910000
Se	4.674987000	-1.657963000	-2.129267000
Cd	5.706268000	0.758737000	-2.179453000
Se	8.341372000	0.578097000	-2.185810000
Cd	-5.200078000	-4.670309000	0.115242000
Se	-2.564972000	-4.850951000	0.108886000
Cd	-1.533690000	-2.434249000	0.058684000
Se	1.101415000	-2.614891000	0.052329000
Cd	1.793488000	-5.149734000	0.098376000
Se	4.428594000	-5.330374000	0.092022000
Cd	5.459876000	-2.913672000	0.041819000
Se	8.094980000	-3.094314000	0.035466000
Cd	-4.691271000	2.756970000	-0.029134000
Se	-2.056165000	2.576329000	-0.035489000
Cd	-1.024883000	4.993031000	-0.085691000
Se	1.610222000	4.812390000	-0.092046000
Cd	2.302295000	2.277546000	-0.045998000
Se	4.937401000	2.096904000	-0.052351000
Cd	5.968682000	4.513607000	-0.102556000
Se	8.603788000	4.332965000	-0.108910000
Cd	-4.937668000	-0.915446000	2.192146000
Se	-2.302563000	-1.096088000	2.185794000
Cd	-1.271281000	1.320614000	2.135575000
Se	1.363824000	1.139973000	2.129224000
Cd	2.055898000	-1.394869000	2.175289000
Se	4.691003000	-1.575511000	2.168937000
Cd	5.722285000	0.841192000	2.118719000
Se	8.357390000	0.660548000	2.112366000
H	-7.664082000	7.801681000	0.768079000
C	-10.167036000	7.014169000	1.537439000
C	-8.500727000	-2.331516000	-0.881506000
S	-8.807505000	-0.730102000	-1.519690000
C	-7.924682000	0.305834000	-0.399263000
S	-6.758735000	-0.869269000	0.284026000
C	-7.479736000	-2.521498000	-0.027089000
S	-7.388848000	-3.884534000	1.071399000
C	-8.838698000	-4.996663000	0.870766000
C	-9.180187000	-5.078125000	-0.616211000
S	-9.741948000	-3.473584000	-1.310177000
C	-8.211133000	1.566141000	-0.136268000
S	-7.187478000	2.603751000	0.865169000
C	-8.051433000	4.112978000	0.610671000
C	-9.175333000	4.032167000	-0.109198000
S	-9.638406000	2.441363000	-0.699124000
C	-9.967361000	-4.479546000	1.733719000
H	-10.087406000	-5.732593000	-0.736743000
H	-8.510452000	-6.002640000	1.236021000
C	-8.045359000	-5.634130000	-1.465104000
S	-7.324986000	5.523785000	1.294470000
S	-10.201477000	5.329145000	-0.609846000
H	-10.278204000	-3.456431000	1.466228000
H	-10.867065000	-5.105880000	1.643180000
H	-9.697409000	-4.461554000	2.798096000
H	-7.565128000	-6.508929000	-0.996622000
H	-8.414036000	-5.963205000	-2.450319000
H	-7.256079000	-4.886055000	-1.680832000
C	-9.513443000	6.838477000	0.181754000
C	-7.989562000	6.868059000	0.228816000
H	-9.939821000	6.195488000	2.237935000

H	-11.264496000	7.060709000	1.462160000
H	-9.850789000	7.946025000	2.028538000
H	-9.860985000	7.655934000	-0.513179000
C	-7.325774000	6.812897000	-1.133243000
H	-7.549865000	7.709739000	-1.731788000
H	-7.649408000	5.950880000	-1.735688000
H	-6.232164000	6.759965000	-1.051493000

Figure 4a (main manuscript) cartesian coordinates $Cd_{16}Se_{16}$-(*S*)-**1** singlet PM6 partial optimization:

Cd	-5.043170000	-0.850427000	-1.977031000
Se	-2.406888000	-0.960420000	-2.096899000
Cd	-1.426722000	1.458785000	-1.791564000
Se	1.209559000	1.348794000	-1.911433000
Cd	1.953521000	-1.142347000	-2.295165000
Se	4.589803000	-1.252339000	-2.415035000
Cd	5.569968000	1.166865000	-2.109699000
Se	8.206250000	1.056874000	-2.229569000
Cd	-5.136250000	-4.835605000	-0.367341000
Se	-2.499967000	-4.945597000	-0.487210000
Cd	-1.519802000	-2.526389000	-0.181890000
Se	1.116480000	-2.636382000	-0.301758000
Cd	1.860441000	-5.127526000	-0.685471000
Se	4.496724000	-5.237517000	-0.805339000
Cd	5.476888000	-2.818309000	-0.500018000
Se	8.113169000	-2.928303000	-0.619885000
Cd	-4.781948000	2.529887000	0.666202000
Se	-2.145665000	2.419895000	0.546333000
Cd	-1.165501000	4.839103000	0.851654000
Se	1.470782000	4.729111000	0.731786000
Cd	2.214742000	2.237966000	0.348073000
Se	4.851025000	2.127972000	0.228207000
Cd	5.831189000	4.547182000	0.533525000
Se	8.467472000	4.437189000	0.413658000
Cd	-4.875032000	-1.455295000	2.275888000
Se	-2.238750000	-1.565289000	2.156023000
Cd	-1.258586000	0.853922000	2.461327000
Se	1.377696000	0.743929000	2.341462000
Cd	2.121658000	-1.747217000	1.957768000
Se	4.757940000	-1.857211000	1.837902000
Cd	5.738104000	0.562001000	2.143207000
Se	8.374386000	0.452006000	2.023340000
H	-6.863733000	7.737548000	-1.272878000
C	-8.729657000	6.985178000	0.574661000
C	-9.048769000	-2.153054000	0.307256000
S	-9.867192000	-0.740215000	-0.411530000
C	-8.464665000	0.325432000	-0.497856000
S	-6.989988000	-0.585629000	-0.244309000
C	-7.684015000	-2.086333000	0.361399000
S	-6.506228000	-3.144267000	1.101627000
C	-7.635512000	-4.108305000	2.253195000
C	-8.831728000	-4.690053000	1.497742000
S	-10.023981000	-3.435150000	0.895577000
C	-8.421420000	1.620439000	-0.663605000
S	-6.889764000	2.496552000	-0.778232000
C	-7.606458000	4.092995000	-1.075303000
C	-8.981459000	4.153447000	-1.139984000
S	-9.826214000	2.663754000	-0.905316000
C	-7.994157000	-3.226938000	3.445618000

H	-9.450140000	-5.285159000	2.221943000
H	-6.969014000	-4.941634000	2.581850000
C	-8.418586000	-5.578790000	0.337762000
S	-6.500328000	5.406879000	-1.193441000
S	-9.934792000	5.549177000	-1.444467000
H	-8.747460000	-2.468231000	3.188769000
H	-8.394045000	-3.809676000	4.271594000
H	-7.104499000	-2.688857000	3.806981000
H	-7.662376000	-6.325094000	0.642374000
H	-9.275013000	-6.126544000	-0.076611000
H	-7.978196000	-4.999183000	-0.499677000
C	-8.845909000	6.935950000	-0.941287000
C	-7.489993000	6.895252000	-1.624446000
H	-8.274621000	6.094667000	1.003079000
H	-9.747249000	7.064308000	1.041334000
H	-8.167909000	7.855545000	0.918668000
H	-9.405729000	7.843571000	-1.305446000
C	-7.597759000	6.961372000	-3.160615000
H	-8.097770000	7.885612000	-3.478815000
H	-8.164619000	6.123909000	-3.583426000
H	-6.597822000	6.945386000	-3.633685000

Figure S10b cartesian coordinates Cd$_{16}$Se$_{16}$-(*S*)-**1** quintet PM6 partial optimization:

Cd	-5.278802000	0.735898000	1.075730000
Se	-2.672346000	0.953993000	1.443523000
Cd	-1.597621000	-1.444216000	1.451980000
Se	1.008834000	-1.226123000	1.819773000
Cd	1.638731000	1.314720000	2.051853000
Se	4.245186000	1.532814000	2.419647000
Cd	5.319911000	-0.865394000	2.428104000
Se	7.926367000	-0.647301000	2.795898000
Cd	-5.322608000	4.562529000	-0.882939000
Se	-2.716151000	4.780622000	-0.515147000
Cd	-1.641429000	2.382413000	-0.506674000
Se	0.965027000	2.600507000	-0.138882000
Cd	1.594925000	5.141351000	0.093180000
Se	4.201382000	5.359444000	0.460971000
Cd	5.276104000	2.961234000	0.469443000
Se	7.882560000	3.179328000	0.837233000
Cd	-4.655376000	-2.846016000	-1.218320000
Se	-2.048919000	-2.627922000	-0.850528000
Cd	-0.974197000	-5.026132000	-0.842055000
Se	1.632260000	-4.808038000	-0.474263000
Cd	2.262157000	-2.267194000	-0.242202000
Se	4.868614000	-2.049099000	0.125588000
Cd	5.943335000	-4.447310000	0.134062000
Se	8.549793000	-4.229216000	0.501853000
Cd	-4.699187000	0.980619000	-3.176987000
Se	-2.092730000	1.198714000	-2.809199000
Cd	-1.018010000	-1.199497000	-2.800710000
Se	1.588447000	-0.981403000	-2.432921000
Cd	2.218346000	1.559441000	-2.200878000
Se	4.824803000	1.777536000	-1.833089000
Cd	5.899524000	-0.620676000	-1.824601000
Se	8.505980000	-0.402580000	-1.456811000
H	-7.484013000	0.085482000	-5.486764000
C	-9.969937000	-0.569182000	-4.568217000
C	-8.281174000	-1.299353000	4.516702000
S	-9.148890000	-1.910639000	3.108574000

C	-8.498691000	-0.757393000	1.964610000
S	-7.582901000	0.531668000	2.759500000
C	-7.540010000	-0.199344000	4.353656000
S	-6.573516000	0.620750000	5.526406000
C	-7.285164000	0.050171000	7.120121000
C	-7.367738000	-1.470468000	7.192931000
S	-8.535739000	-2.193774000	5.972583000
C	-8.570157000	-0.811309000	0.637793000
S	-7.804329000	0.449097000	-0.344542000
C	-7.848951000	-0.413561000	-1.908433000
C	-8.522875000	-1.567796000	-1.857295000
S	-9.268809000	-2.068882000	-0.352541000
C	-8.605550000	0.749075000	7.365839000
H	-7.838121000	-1.754928000	8.177651000
H	-6.525690000	0.404623000	7.874058000
C	-6.025867000	-2.159846000	7.057821000
S	-7.127350000	0.474500000	-3.193911000
S	-8.754359000	-2.626110000	-3.202646000
H	-9.377387000	0.494314000	6.624680000
H	-9.022380000	0.496031000	8.351958000
H	-8.501051000	1.844535000	7.342941000
H	-5.319491000	-1.829123000	7.834598000
H	-6.109593000	-3.252226000	7.159248000
H	-5.535955000	-1.970392000	6.091424000
C	-8.736416000	-1.448715000	-4.610344000
C	-7.432016000	-0.667393000	-4.659713000
H	-9.960305000	0.130364000	-3.718247000
H	-10.894960000	-1.157039000	-4.489654000
H	-10.056806000	0.047240000	-5.473860000
H	-8.793622000	-2.124104000	-5.508076000
C	-6.205577000	-1.552638000	-4.827571000
H	-6.324977000	-2.267390000	-5.653555000
H	-5.983102000	-2.143719000	-3.918970000
H	-5.305640000	-0.951300000	-5.064887000

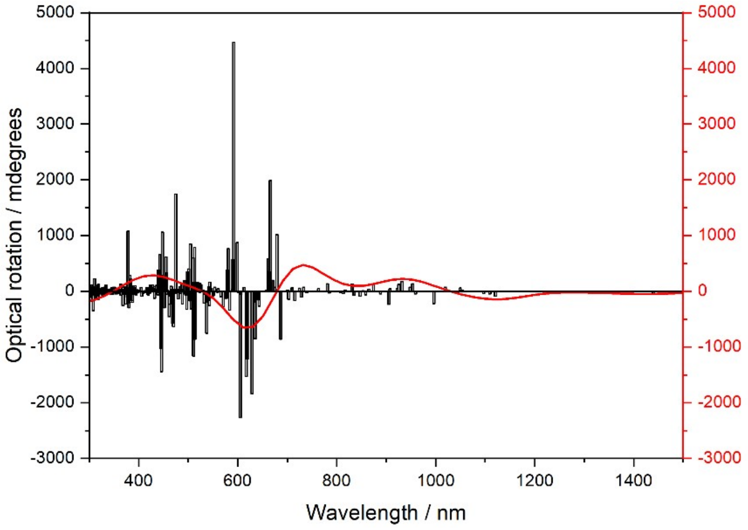

Figure S11. Theoretically calculated CD emission (luminescence) spectrum, rotational strength of $Cd_{16}Se_{16}$:(*S*)-**1**, triplet state.

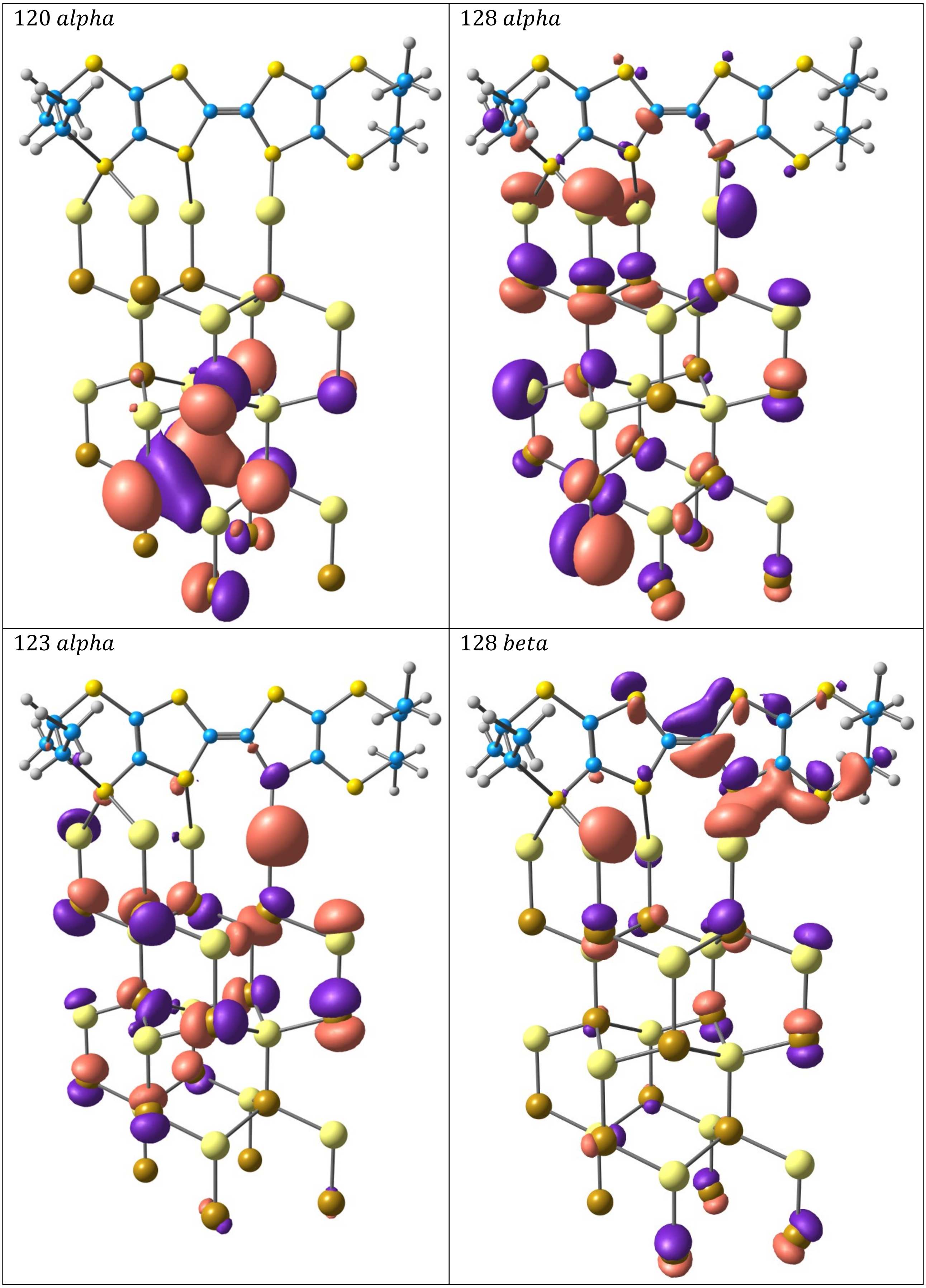

120 *alpha*

128 *alpha*

123 *alpha*

128 *beta*

Figure S12. Cd$_{16}$Se$_{16}$:(*S*)-**1** triplet state, the shape of molecular orbitals MOs involved with the higher weight in the 635.0 nm electronic transition are shown: molecular orbital number 120 and 128 (alpha), 123 and 128 (beta), noting that MOs 123 and 124 are the HOMO and LUMO. In particular single particle electronic transitions are: 120A→128A (0.17517), $123B \rightarrow 128B\ (0.17182)$, where numbers in parenthesis are the weight of the transition in the overall 635.0 nm excitation.

References

1 E. Kaxiras, *Atomic and Electronic Structure of Solids - Cambridge University Press*, Cambridge University Press, 2003.

2 J. J. P. Stewart, *J Mol Model*, 2008, **14**, 499–535.

3 K. L. Sowers, Z. Hou, J. J. Peterson, B. Swartz, S. Pal, O. Prezhdo and T. D. Krauss, *Chemical Physics*, 2016, **471**, 24–31.

4 D. K. Freeman, S. L. Mair and Z. Barnea, *Acta Crystallographica Section A*, 1977, **33**, 355–359.

5 S. S. Zumdahl, *Chemical Principles 6th Ed. Houghton Mifflin Company.*, Houghton Mifflin Company, 2009, pA21.